Polar magneto-optical Kerr effect for low-symmetric ferromagnets

Helmut Rathgen,[1,2,*] Mikhail I. Katsnelson,[2,3] Olle Eriksson,[2] and Gertrud Zwicknagl[1]
[1]*Institut für Mathematische Physik, Technische Universität Braunschweig, Mendelssohnstraße 3, D-38106 Braunschweig, Germany*
[2]*Condensed Matter Theory, Department of Physics, Uppsala University, Box 530, S-75121 Uppsala, Sweden*
[3]*Institute for Molecules and Materials, Radboud University Nijmegen, Toernooiveld 1, 6525 ED, The Netherlands*
(Received 2 November 2004; revised manuscript received 6 April 2005; published 20 July 2005)

The polar magneto-optical Kerr effect (MOKE) for low-symmetric ferromagnetic crystals is investigated theoretically based on first-principles calculations of optical conductivities and a transfer matrix approach for the electrodynamics part of the problem. Exact average magneto-optical properties of polycrystals are described, taking into account realistic models for the distribution of domain orientations. It is shown that for low-symmetric ferromagnetic single crystals the MOKE is determined by an interplay of crystallographic birefringence and magnetic effects. Calculations for a single crystal and bicrystal of hcp $\langle 11\bar{2}0\rangle$ Co and for a polycrystal of CrO_2 are performed, with results being in good agreement with experimental data.

DOI: 10.1103/PhysRevB.72.014451 PACS number(s): 78.20.Bh, 78.20.Ci

I. INTRODUCTION

The magneto-optical Kerr effect (MOKE) is a versatile method to probe the magnetic properties of thin films. Advanced by the rapid developments in crystallographic growth techniques, a variety of low-symmetric crystalline surfaces have been subject to MOKE measurements in the last decades. This has led to systematic investigations of magneto-optical anisotropy effects.[1]

State-of-the-art theoretical approaches to investigate the MOKE are based on first-principles calculations of dielectric tensors in the framework of the Kubo-Greenwood formalism[2,3] as suggested by Wang and Callaway.[4] The MOKE is obtained from a dielectric tensor by means of an approximative analytic expression

$$\psi + i\chi = \frac{\varepsilon_{xy}}{(1-\varepsilon_{xx})\sqrt{\varepsilon_{xx}}} \tag{1}$$

derived originally by Argyres in 1955.[5] ψ denotes the Kerr rotation and χ denotes the Kerr ellipticity.

This approach requires in general that the dielectric tensor has symmetry

$$\varepsilon = \begin{pmatrix} \varepsilon_{xx} & \varepsilon_{xy} & 0 \\ -\varepsilon_{xy} & \varepsilon_{xx} & 0 \\ 0 & 0 & \varepsilon_{zz} \end{pmatrix}. \tag{2}$$

There have been theoretical attempts to extend the approach to low-symmetric systems. However, so far a complete electrodynamics calculation for low-symmetric dielectric tensors has not been considered.

There are many interesting ferromagnets that have a low symmetry: e.g., CrO_2, hcp $\langle 11\bar{2}0\rangle$ Co, and FePt grown in the $\langle 010\rangle$ direction. All of these systems have two different crystallographic axes in the surface plane, so beside their magneto-optical activity they exhibit crystallographic birefringence.

In this paper we show that for such crystals it is important to consider the complete optical response including birefringence and magnetic effects in order to describe correctly the polar MOKE. Further, we show that the optical response is qualitatively different for single crystals and polycrystals and, finally, for polycrystals it sensitively depends on the ordering of crystallographic domains. We calculate the MOKE of hcp $\langle 11\bar{2}0\rangle$ Co and of $\langle 010\rangle$ CrO_2. For Co we show that the previous interpretation of experimental data of anisotropic polar MOKE (Ref. 1) in terms of a manifestation of magnetocrystalline anisotropy remains valid.

The paper is organized as follows. In the subsequent section we describe our approach to the complete calculation of the electrodynamics problem by means of transfer matrix methods. A theoretical description of ellipsometry measurements for single crystals and polycrystals is given in Sec. III. In Sec. IV we discuss first-principles calculations of optical conductivities. The space-time symmetry of Co and CrO_2 crystals is described in Sec. V. The calculated optical response of Co and CrO_2 is presented in Secs. VI and VII, respectively. In Sec. VIII a summary and conclusions are given.

II. TRANSFER MATRIX METHODS

The optical response of a finite system of layers to an incident plane wave can be described by transfer matrix methods.[6–8] The description is valid if the magnetic permeability is unity and the wavelength of the light is large compared to the microscopic structure of materials and also large compared to interface roughness. In the most general case a system with n boundaries is described by a regular set of $4n$ linear equations that determines the complex amplitude vectors of all plane waves in all media. We briefly describe the method.

We first choose a coordinate system such that the z axis is the surface normal and the scattering plane is spanned by the z and y axes. In the half space of the incident and reflected wave Fresnel's secular equation reads

$$-\boldsymbol{k}^2\boldsymbol{E}+\frac{\omega^2}{c^2}\varepsilon\boldsymbol{E}=\boldsymbol{0}. \tag{3}$$

We substitute $\boldsymbol{r}\mapsto(\omega/c)\boldsymbol{r}$ and define $q:=(c/\omega)k_y$ and $k:=(c/\omega)k_z$. This gives

$$q=\sqrt{\varepsilon}\sin\vartheta,$$

$$k=\pm\sqrt{\varepsilon}\cos\vartheta=:\pm k_0, \tag{4}$$

where ϑ is the incident angle. This gives an ansatz for the wave,

$$\boldsymbol{E}=\boldsymbol{E}^{in}e^{i(qy-k_0z-\omega t)}+E^{refl}e^{i(qy+k_0z-\omega t)}, \tag{5}$$

where $\boldsymbol{E}^{in}$ is the known amplitude vector of the incident wave and the complex amplitude vector of the reflected wave satisfies

$$E_z^{refl}=-\frac{q}{k_0}E_y^{refl}, \tag{6}$$

leaving two free parameters E_x^{refl} and E_y^{refl}. For other media the most general plane-wave solution to Maxwell's equations is a combination of four independent waves. In the case of a scalar medium it is

$$\boldsymbol{E}=\boldsymbol{E}^1e^{i(qy+k^1z-\omega t)}+\boldsymbol{E}^2e^{i(qy+k^2z-\omega t)}, \tag{7}$$

where

$$k^{1,2}=\pm\sqrt{\varepsilon-q^2} \tag{8}$$

and the x and y components of $\boldsymbol{E}^1$ and $\boldsymbol{E}^2$ are independent. In the case of a tensor medium it is

$$\boldsymbol{E}=a^1\boldsymbol{n}^1e^{i(qy+k^1z-\omega t)}+\cdots+a^4\boldsymbol{n}^4e^{i(qy+k^4z-\omega t)}, \tag{9}$$

with four free parameters $a^1,\ldots,a^4$ satisfying

$$\boldsymbol{E}^i=a^i\boldsymbol{n}^i. \tag{10}$$

$k^1,\ldots,k^4$ are the roots of the fourth-order polynomial in k,

$$\mathrm{Det}\begin{vmatrix}\varepsilon_{xx}-q^2-k^2 & \varepsilon_{xy} & \varepsilon_{xz}\\ \varepsilon_{yx} & \varepsilon_{yy}-k^2 & \varepsilon_{yz}+qk\\ \varepsilon_{zx} & \varepsilon_{zy}+qk & \varepsilon_{zz}-q^2\end{vmatrix}=0, \tag{11}$$

and the vectors $\boldsymbol{n}^1,\ldots,\boldsymbol{n}^4$ are associated kernels.

In the half space on the backside of the layers two waves can always be discarded. For a transparent medium these are two backward-traveling waves; for an absorbing medium these are two exponentially decaying waves.

In our case (a bulk metallic system with no intermediate layer) we have only an absorbing tensor half space and the ansatz for the waves in the responding system reduces to

$$\boldsymbol{E}=a^1\boldsymbol{n}^1e^{i(qy+k^1z-\omega t)}+a^2\boldsymbol{n}^2e^{i(qy+k^2z-\omega t)}, \tag{12}$$

where k^1 and k^2 are the roots that have negative imaginary parts (negative z direction corresponds to forward-traveling waves).

Stressing the assumption of unity magnetic permeability, four independent boundary conditions follow from Maxwell's equations stating that

$$E_x,E_y,\partial_zE_x \quad\text{and}\quad iqE_z-\partial_zE_y \tag{13}$$

are continuous.

Substituting the ansatz, Eqs. (5) and (12), in the boundary conditions, we get

$$\begin{pmatrix}-1 & 0 & n_x^1 & n_x^2\\ 0 & -1 & n_y^1 & n_y^2\\ -k_0 & 0 & k^1n_x^1 & k^2n_x^2\\ 0 & \frac{q^2}{k_0}+k_0 & qn_z^1-k^1n_y^1 & qn_z^2-k^2n_y^2\end{pmatrix}\begin{pmatrix}E_x^{refl}\\ E_y^{refl}\\ a^1\\ a^2\end{pmatrix}=\begin{pmatrix}E_x^{in}\\ E_y^{in}\\ -k_0E_x^{in}\\ qE_z^{in}+k_0E_y^{in}\end{pmatrix}. \tag{14}$$

This is a regular system of four linear equations. Stressing Eqs. (6) and (10) its solution determines the complex amplitudes vectors of all waves.

We have written a numerical implementation of the most general case of a transfer matrix approach [based on standard LAPACK (Ref. 9) routines and polynomial solver[10]]. It is described in detail in Ref. 11.

III. ELLIPSOMETRY FOR SINGLE CRYSTALS AND POLYCRYSTALS

The state of polarization of a plane wave is conveniently described by Stokes parameters[6]

$$\boldsymbol{S}=\begin{pmatrix}S_0\\ S_1\\ S_2\\ S_3\end{pmatrix}=\begin{pmatrix}E_x\bar{E}_x+\bar{E}_yE_y\\ E_x\bar{E}_x-\bar{E}_yE_y\\ E_x\bar{E}_y+\bar{E}_xE_y\\ i(E_x\bar{E}_y-\bar{E}_xE_y)\end{pmatrix}, \tag{15}$$

where $\boldsymbol{E}=(E_x,E_y)$ is the complex amplitude vector of the plane wave in the coordinate system of the polarization state analysis.

The state of polarization of a set of incoherent plane waves that add by their intensities is described by the sum of their Stokes parameters. Both for a single wave and for an incoherent wave, the rotation angle of the polarization ellipse ψ and its ellipticity χ are related to the Stokes parameters by

$$\tan 2\psi=\frac{S_2}{S_1} \tag{16}$$

and

$$\sin 2\chi=\frac{S_3}{\sqrt{S_1^2+S_2^2+S_3^2}}. \tag{17}$$

In the general case the polarization ellipse is the intensity behind an analyzer for all positions. Only in the special case

of a single wave is this equivalent to the curve that is drawn by the tip of the electric field vector.

The optical response of a polycrystal can be described by the sum over Stokes parameters of single-crystalline domains weighted by surface areas of the domains and intensities shining on them.[12] The sum extends over all domains that are illuminated in the experiment. The approach is valid if single-crystalline domains are large compared to the wavelength. We can calculate Stokes parameters for polycrystals by summing over Stokes parameters obtained from transfer matrix calculations for single crystals.

IV. FIRST-PRINCIPLES CALCULATIONS OF OPTICAL CONDUCTIVITIES

We briefly describe the calculation of optical constants by means of first-principles calculations. Our approach is basically standard unless we evaluate the Kubo-Greenwood formula directly without a Kramers-Kronig transformation and analytical continuation (see also Ref. 13).

In this section we consider the optical conductivity tensor σ rather than the corresponding dielectric tensor ε. The quantities are related by the identity

$$\varepsilon_{\alpha\beta}(\omega) = \delta_{\alpha\beta} + i\frac{4\pi}{\omega}\sigma_{\alpha\beta}(\omega). \tag{18}$$

In general, intraband, as well as direct and indirect interband, transitions contribute to the optical conductivity. Spins may flip (for magnetic dipole transitions) or stay constant (for electric dipole transitions) during excitations. It is a common practice to account only for the contribution of electric dipole (non-spin-flip) direct interband transitions by means of *ab initio* methods while treating the contribution of intraband transitions by a phenomenological Drude term

$$\sigma_D(\omega) = \frac{\sigma_0}{1+\omega^2\tau^2} \tag{19}$$

and neglecting all other contributions.[4,14–16] A broad variety of linear optical and magneto-optical effects in metals as well as in semiconductors have been successfully described in the framework of this approximation; see, e.g., Refs. 17 and 18 and references therein. In the transition metals, intraband transitions turn out to be important in the range from 0 eV up to 0.5 eV.[19] It is shown in Ref. 4 that a corresponding Drude contribution is negligible for energies larger than 1 eV in the case of Ni. Throughout this work we neglect any phenomenological Drude contribution.

The Kubo-Greenwood expression for the contribution of direct interband transitions to the optical conductivity reads[14]

$$\sigma_{\alpha\beta}(\omega) = \frac{ie^2}{m^2\hbar}\int_{BZ} d^3k \sum_{\substack{l,n \\ E_l(\mathbf{k})<E_F \\ E_n(\mathbf{k})>E_F}} \frac{1}{\omega_{nl}(\mathbf{k})}\left[\frac{\Pi^\alpha_{ln}(\mathbf{k})\Pi^\beta_{nl}(\mathbf{k})}{\omega-\omega_{nl}(\mathbf{k})+\frac{i}{\tau(\omega)}} + \frac{(\Pi^\alpha_{ln}(\mathbf{k})\Pi^\beta_{nl}(\mathbf{k}))^*}{\omega+\omega_{nl}(k)+\frac{i}{\tau(\omega)}}\right], \tag{20}$$

where the indices l and n denote the spin and all band quantum numbers for the occupied and empty states, respectively, $\boldsymbol{k}$ is the quasimomentum running through the Brillouin zone, and E_F is the Fermi energy. The symbol $\Pi^\alpha_{nl}(\boldsymbol{k})$, $\alpha=x,y,z$, denotes the matrix elements of the momentum operator given below by Eq. (22), and $\omega_{nl}(\boldsymbol{k})$ is the energy difference between the involved states,

$$\omega_{nl}(\boldsymbol{k}) = \frac{1}{\hbar}[E_n(\boldsymbol{k}) - E_l(\boldsymbol{k})]. \tag{21}$$

Finally, $\tau(\omega)$ is a phenomenological relaxation time. Throughout this work we use a constant relaxation time of 0.136 eV. The results of this paper are insensitive to the actual choice of this value.

Together with the energy differences $\omega_{nl}(\boldsymbol{k})$, the matrix elements of the momentum operator are obtained from the underlying band structure calculation by evaluating the expression

$$\boldsymbol{\Pi}_{ln}(\boldsymbol{k}) = \int d^3r\,\psi^*_l(\boldsymbol{k},\boldsymbol{r})\left[\boldsymbol{p} + \frac{\hbar}{4mc^2}[\boldsymbol{\sigma}\times\boldsymbol{\nabla}V(\boldsymbol{r})]\right]\psi_n(\boldsymbol{k},\boldsymbol{r}). \tag{22}$$

Here $\psi_n(\boldsymbol{k},\boldsymbol{r})$ is the Bloch wave function with quantum numbers as described above, $\boldsymbol{p}=-i\hbar\nabla$, and $V(\boldsymbol{r})$ is a crystal potential. State-of-the-art works on *ab initio*–calculated optical constants neglect the spin-orbit term in the expression for the matrix elements of the momentum operator, Eq. (22). This has been found to be a good approximation; see, e.g., Ref. 4. We follow this approach.

Expression (20) may be computed directly or via symmetrized limit expressions requiring Kramers-Kronig transformations and analytical continuation to finite relaxation times. We recently discussed the advantages and disadvantages of both approaches that become important when the conductivity tensor has low symmetry.[13] In the present paper expression (20) is computed directly.

For electronic structure calculation we use a relativistic full-potential linear muffin-tin orbital (FP-LMTO) code. The code is described in detail in Ref. 20. A discussion of the treatment of spin-orbit coupling by means of the second variational step can be found in Ref. 21.

V. SYMMETRY CONSIDERATIONS

We have used standard space-time symmetry analysis[22] to find the irreducible forms of the dielectric tensors of hcp Co with magnetization along $\langle 11\bar{2}0\rangle$ and of CrO_2 with magnetization along $\langle 010\rangle$. The crystal structures are

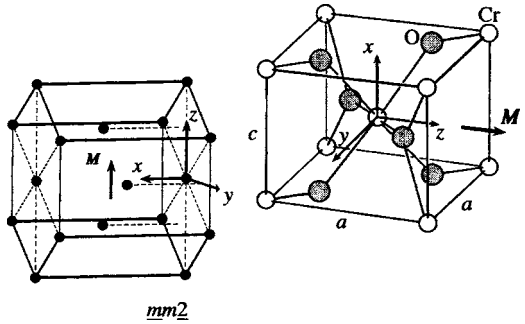

FIG. 1. Crystal structures of (a) $\langle 11\bar{2}0\rangle$ ferromagnetic hcp Co and (b) $\langle 010\rangle$ ferromagnetic CrO_2. Coordinate systems are as used in magneto-optics calculations.

shown in Fig. 1. We find space-time point groups $\underline{m}m\underline{2}$ and $\underline{2}/\underline{m}$ for Co and CrO_2, respectively. Making the coordinate systems explicit, irreducible sets of point group operations can be chosen as *identity, twofold rotation around z followed by space inversion* and *twofold rotation around y followed by time inversion* for Co and *identity, space inversion*, and *twofold rotation around x followed by time inversion* for CrO_2. Standard symbols are 1, $\bar{2}z$, $\underline{2}y$ and 1, $\bar{1}$, $\underline{2}x$, respectively.

Irreducible space-time symmetries of the dielectric tensors follow by Neumann's principle which states that

$$\varepsilon = \sigma \circ \varepsilon \circ \sigma^{-1} \tag{23}$$

has to be satisfied for any symmetry operator σ. For classical point-group operators the respective matrix equation can be evaluated. For nonclassical operators $\sigma = s \circ \tau$ composed of a classical operator s and the time inversion operator τ, Eq. (23) can be brought into matrix form by stressing the equivalence of time inversion and magnetization reversal,

$$\tau \circ \varepsilon(\boldsymbol{M}) \circ \tau^{-1} = \varepsilon(-\boldsymbol{M}), \tag{24}$$

and Onsager's relation

$$\varepsilon(-\boldsymbol{M}) = \varepsilon^{T}(\boldsymbol{M}), \tag{25}$$

where T denotes the transpose.

For the Co crystal we find

$$\varepsilon = \begin{pmatrix} \varepsilon_{xx} & \varepsilon_{xy} & 0 \\ -\varepsilon_{xy} & \varepsilon_{yy} & 0 \\ 0 & 0 & \varepsilon_{zz} \end{pmatrix}. \tag{26}$$

For CrO_2 we have

$$\varepsilon = \begin{pmatrix} \varepsilon_{xx} & \varepsilon_{xy} & \varepsilon_{xz} \\ -\varepsilon_{xy} & \varepsilon_{yy} & \varepsilon_{yz} \\ -\varepsilon_{xz} & \varepsilon_{yz} & \varepsilon_{zz} \end{pmatrix}. \tag{27}$$

Next we consider the symmetry properties of the same crystals but without magnetism. Co has the well-known point group $6/mmm$, and the irreducible form of the dielectric tensor without magnetism is

$$\varepsilon = \begin{pmatrix} \varepsilon_{xx} & 0 & 0 \\ 0 & \varepsilon_{yy} & 0 \\ 0 & 0 & \varepsilon_{yy} \end{pmatrix}. \tag{28}$$

The CrO_2 crystal without magnetism is *nonsymmomorphic*. It has space group $P4_2/mmm$. Evaluation of Neumann's principle is standard for pure point group operators. For symmetry operators $\hat{\sigma} = \sigma \circ T$, which are a combination of a point-group operator σ and the translation operator T [the fourfold screw axis $4x \circ T(c/2,0,0)$ in our case], Neumann's principle can be evaluated by stressing the invariance of the dielectric tensor under arbitrary translations:

$$T \circ \varepsilon \circ T^{-1} = \varepsilon. \tag{29}$$

We find the irreducible form of the dielectric tensor without magnetism is the same as for Co.

Next we consider the expansion of the dielectric tensor in powers of the magnetization and stress the following symmetry properties: The zeroth-order contribution has symmetry of the nonmagnetic crystal. Magnetic contributions of odd order have space-time symmetry of the magnetic crystal and are antisymmetric. Magnetic contributions of even order have space-time symmetry of the magnetic crystal and are symmetric. The antisymmetry and symmetry properties, respectively, of odd and even-order magnetic contributions are arrived at in general by applying Onsager's relation to the expansion.

We find that up to second order in the magnetization the expansion has the symmetry, for Co,

$$\varepsilon = \begin{pmatrix} \varepsilon^0_{xx} & 0 & 0 \\ 0 & \varepsilon^0_{yy} & 0 \\ 0 & 0 & \varepsilon^0_{yy} \end{pmatrix} + \begin{pmatrix} 0 & \varepsilon^1_{xy} & 0 \\ -\varepsilon^1_{xy} & 0 & 0 \\ 0 & 0 & 0 \end{pmatrix} + \begin{pmatrix} \varepsilon^2_{xx} & 0 & 0 \\ 0 & \varepsilon^2_{yy} & 0 \\ 0 & 0 & \varepsilon^2_{zz} \end{pmatrix} \tag{30}$$

and, for CrO_2,

$$\varepsilon = \begin{pmatrix} \varepsilon^0_{xx} & 0 & 0 \\ 0 & \varepsilon^0_{yy} & 0 \\ 0 & 0 & \varepsilon^0_{yy} \end{pmatrix} + \begin{pmatrix} 0 & \varepsilon^1_{xy} & \varepsilon^1_{xz} \\ -\varepsilon^1_{xy} & 0 & 0 \\ -\varepsilon^1_{xz} & 0 & 0 \end{pmatrix} + \begin{pmatrix} \varepsilon^2_{xx} & 0 & 0 \\ 0 & \varepsilon^2_{yy} & \varepsilon^2_{yz} \\ 0 & \varepsilon^2_{yz} & \varepsilon^2_{zz} \end{pmatrix}. \tag{31}$$

Results of standard electronic structure calculations are for both systems tensors of the form[12,23,24] (see also Secs. VI A and VII A)

$$\varepsilon = \begin{pmatrix} \varepsilon_{xx} & \varepsilon_{xy} & 0 \\ -\varepsilon_{xy} & \varepsilon_{yy} & 0 \\ 0 & 0 & \varepsilon_{yy} \end{pmatrix}. \tag{32}$$

This has an important implication. It means that the second-order magnetic contribution (which would appear as, e.g., a difference between ϵ_{yy} and ϵ_{zz}) is either absent in both systems or *not* resolvable with standard electronic structure calculations. There is no reason why the second-order magnetic contribution should be absent. So basically the conclusion is that it is not resolvable with standard electronic structure calculations. We discuss this in more detail in Sec. VI.

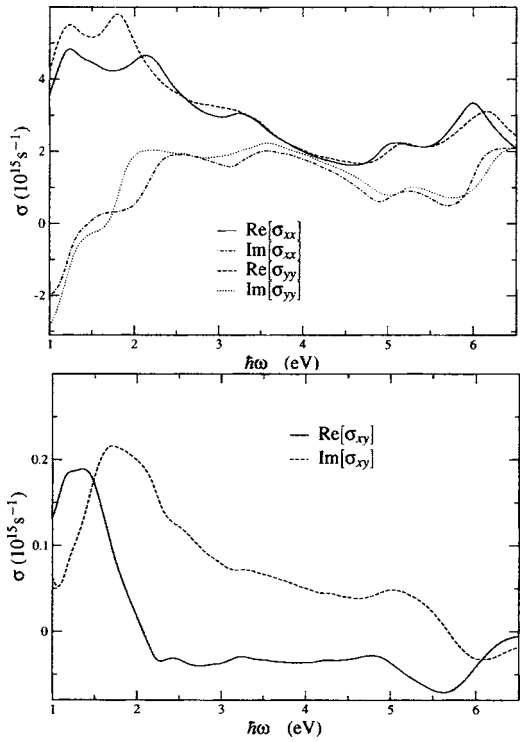

FIG. 2. Calculated optical conductivity tensor of hcp Co with magnetization direction $\langle 11\bar{2}0\rangle$. Quantities are shown in a range where only direct interband tranzition are important.

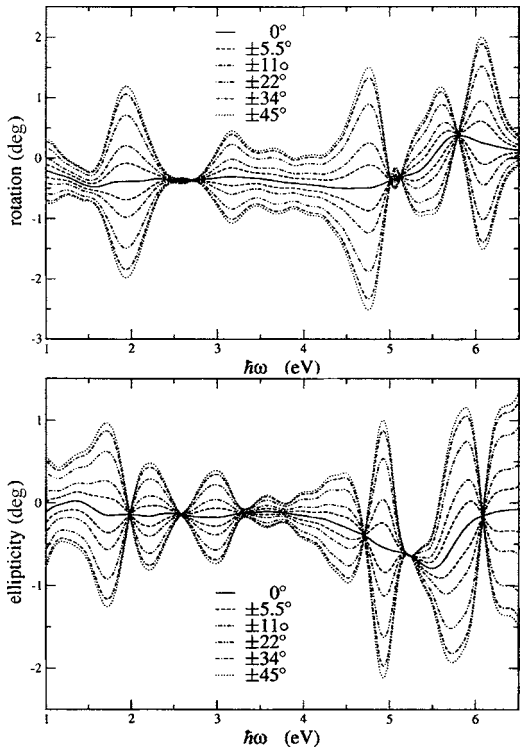

FIG. 3. Calculated optical response of $\langle 11\bar{2}0\rangle$ hcp Co in polar MOKE geometry. The polarization vector is parallel to the crystallographic x axis at zero angle. Curves shifted to higher values just below 5 eV correspond to positive angles.

For the case of CrO_2 we conclude that ϵ_{xz} is actually zero in the first-order magnetic contribution. However, it might still be present in the third order.

VI. POLAR MOKE OF $\langle 11\bar{2}0\rangle$ hcp Co

A. Optical conductivity

We have calculated the optical conductivity tensor of hcp $\langle 11\bar{2}0\rangle$ Co. A hybridized $4s4p3d$ and $5s5p4d$ basis was used in the calculations to describe the Co atoms. Exchange correlation was taken into account in the framework of the local spin density approximation in the form proposed in Ref. 25. The lattice constants were $a=2.5071$ Å and $c=4.0695$ Å. Here 38 400 **k** points were used to sample the Brillouin zone. Results are shown in Fig. 2. They are in good agreement with previous theoretical results.[23,24] In the output of the calculation we find that tensor elements that should be zero due to symmetry are of the order of 10^9 s^{-1} while we find a difference between σ_{yy} and σ_{zz} of the order of 10^{13} to 10^{12} s^{-1}. Thus the symmetry of our calculated tensor is in agreement with Eqs. (26) and (30). We conclude that the calculated difference between σ_{yy} and σ_{zz} is a signature of a second-order magnetic contribution. However, if we change the numerical parameters of our calculation (e.g., basis set, **k**-point mesh), the variation of σ_{yy} and σ_{zz} is typically larger. So we have to conclude within the error of our calculation σ_{yy} and σ_{zz} are equal. The conclusion is that the second-order magnetic contribution *cannot* be resolved with standard electronic structure calculations.

B. Optical response of the single crystal

We have calculated the optical response in polar MOKE geometry with perpendicular incident light with our transfer matrix approach. We find that the optical response depends strongly on the direction of the polarization vector in the surface plane. If the polarization vector is along one of the main crystal axes, birefringence is absent and the optical response is similar to the common polar MOKE. When the polarization vector is turned away from the main crystal axis the optical response is a combination of crystallographic birefringence and a magnetic effect. We find that birefringence starts to be important at about 3°. Results are shown in Fig. 3. Directions of the polarization vector are in one-quarter of the full circle in the surface plane which is chosen symmetrically around the crystallographic x axis. For directions of the polarization vector chosen around the crystallographic y axis, results are identical on the scale of the plot. The latter is a nontrivial result. Since the crystallographic x and y directions are different, one would expect independent results in half of the full circle. It can only be understood by stressing that the birefringence is large compared to the magnetic effect (see below and Sec. VI D). The solid curves show the case when the polarization vector is parallel to a main crystal axis. The optical response is similar to the polar MOKE of hcp $\langle 0001\rangle$ Co.[23,24] To a good approximation it can be regarded as a common polar MOKE response without birefringence. The dashed and dotted curves show the optical response for cases when birefringence is important. If the polarization vector

has an angle of ±5.5° relative to the main crystal axis, the birefringent contribution has about the same magnitude as the magnetic effect. It reaches its maximum at an angle of ±45°. At this angle it is about one order of magnitude larger than the magnetic effect.

The present system has been investigated experimentally in detail by Weller *et al.*[1] In this experiment different samples were used at least one of which was a polycrystal with two types of crystallographic domains related to each other by a 90° rotation around the surface normal. Experimental results do not report birefringent contributions or a dependence on the direction of the polarization vector. So our theoretical results for the single crystal presented here are very different from experimental findings. Still, there is no direct disagreement between theory and experiment simply because it is possible that the experimental data that were taken actually correspond to the case when the polarization vector is along a main crystal axis. For this case there is good agreement with theory (see Fig. 5). However, we believe that this is not what was happening. Rather we speculate that during measurements at some point different directions of the polarization vector were used and still basically the common polar MOKE was found without substantial dependence on the direction of the polarization vector. Let us for the moment focus on the sample which we know is a polycrystal. Then the conclusion is that the optical response of a polycrystal with two domain orientations is fundamentally different from the optical response of a single crystal, so in order to describe experiment correctly, it is important to consider the full polycrystal rather than a single-crystalline sample.

C. Optical response of the bicrystal

We have calculated the optical response of a polycrystal with two domain orientations. Our approach was to calculate average Stokes parameters from our transfer matrix calculation as described in Sec. III. Experimental data about the distribution of domain sizes and intensities shining on them were not known, so we had to make an assumption here. We expect that crystal growth occurs with equal preferrence in both of the two domain orientations, so the total surface areas should be the same and total intensity of the incident light should be devided equally among the two orientations.

Results are shown in Fig. 4. In general, we find now for any direction of the polarization vector that our calculated optical response is similar to the common polar MOKE and theoretical results are now in good agreement with experimental data. The birefringent contribution, which for the single crystal was the dominant contribution to the optical response, is now averaged out. However, the birefringent contribution is averaged out completely only in the ellipticity (in our computational result variation under change of the direction of the polarization vector is of the order 10^{-4} deg) while in the rotation it is still present.

In general the results are quite surprising: For the single crystal birefringence was about 10 times larger than the magnetic effect. For the polycrystal it is averaged out so strongly that it is now smaller than the magnetic contribution. How is this possible only due to the presence of *one* additional domain orientation? And, second, why is the birefringent contribution completely missing in the ellipticity but still present in the rotation? It is important to find out the general mechanism behind this.

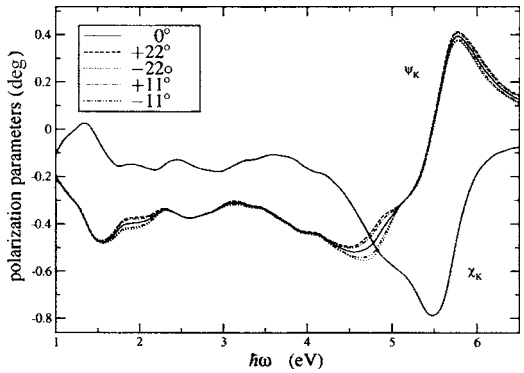

FIG. 4. Calculated optical response of bicrystalline hcp $\langle 11\bar{2}0\rangle$ Co. At 0° the polarization vector is along a main crystal axis of one of the domains.

We have considered average Stokes parameters for polycrystals with ordered domains analytically. We find that the optical response strongly depends on the in-plane symmetry of the domain orientations. In the majority of cases, ordered polycrystals are equivalent to polycrystals with a random domain distribution and thus the optical response is independent of the direction of the polarization vector. In particular we can prove that the Stokes parameters S_0 and S_3 are identical to those of a random polycrystal if and only if the in-plane symmetry of domain orientations is larger than twofold and the Stokes parameters S_1 and S_2 are identical to those of a random polycrystal if and only if the symmetry of domain orientations is not 1, 2, or 4. The proof is given in Appendix A. Analytical findings are in good agreement with the computational result we present here for the hcp $\langle 11\bar{2}0\rangle$ polycrystal with two domains. In particular they explain the different behavior of averaging out in rotation and ellipticity [only S_1 and S_2 enter in the rotation, Eq. (16), while mainly S_3 enters in the ellipticity, Eq. (17); now note that the polycrystal with two domains oriented by a 90° rotation has fourfold symmetry]. The analytical findings have an important consequence for experiments. They imply that if only a few ordered domains are present inside the illuminated area, the optical response will always be very close to the common polar MOKE.

We now conjecture that the second sample that was investigated in experiments [the Ru$(11\bar{2}0)$ sample] was also a polycrystal (the presence of few ordered domains in the illuminated area is enough). For any direction of the polarization vector that was possibly considered in experiment we immediately have agreement with theory. A summarizing comparison of the theoretical data with experiment is shown in Fig. 5. Data for $\langle 0001\rangle$ hcp Co are shown for comparison. The theoretical data for $\langle 0001\rangle$ hcp Co have been calculated in the same way as the data for $\langle 11\bar{2}0\rangle$ hcp.

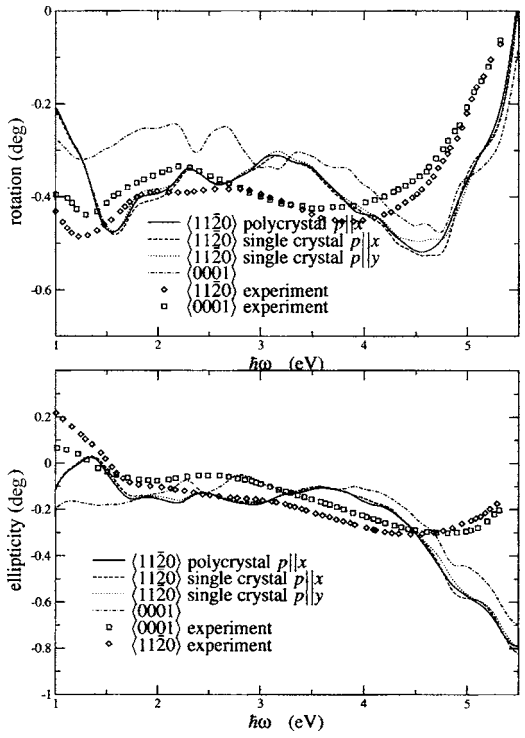

FIG. 5. Optical response of hcp $\langle 11\bar{2}0\rangle$ Co in polar MOKE geometry. Theoretical data are for special cases of the direction of the polarization vector. Experimental data are due to Weller *et al.* Results for hcp $\langle 0001\rangle$ are shown for comparison.

They are is in good agreement with previous theoretical data.[23,24]

D. Anisotropic polar MOKE

The goal of the previous experimental work of Weller and co-workers was to find a manifestation of magnetocrystalline anisotropy in the magneto-optical response. They investigated how the optical response changes when the relative orientation between magnetization and crystal lattice is changed while the polar measuring geometry and other parameters of the experiment are kept (lattice parameters, crystal growth quality, etc.). It was found that the optical response of hcp $\langle 0001\rangle$ and hcp $\langle 11\bar{2}0\rangle$ is different. These results were explained by the dependence of the absorptive part of the refractive index on the angle between crystallographic c axis and spin moment.

We know now that the electrodynamics part of the problem is much more complicated. It is important to calculate the full optical response including crystallographic birefringence and also the polycrystalline nature of the sample has to be taken into account. So it is important to check if the main conclusions given in the experimental work still hold. As we will see below, the answer is yes.

From a theoretical point of view the situation is the following: We have the common polar MOKE in hcp $\langle 0001\rangle$ (no birefringence, optical response is independent of direction of the polarization vector) and a combination of birefringence and magnetic response with strong averaging out of birefringence in the hcp $\langle 11\bar{2}0\rangle$ polycrystal. So the optical responses are fundamentally different. Nevertheless, in both systems the magnetic contribution to the optical response originates from the tensor element ε_{xy}. We would say that we have measured anisotropy in the magneto-optical constants if we can conclude from the measurement that ε_{xy} has changed due to a change of the magnetization direction. So what we want to show now is that the difference in the magneto-optical response between single-crystalline hcp $\langle 0001\rangle$ and polycrystalline hcp $\langle 11\bar{2}0\rangle$ is basically only determined by the change in ε_{xy}. Admittedly we do not think this can be proven rigorously. However, what we can do is to calculate the optical response of the hcp $\langle 11\bar{2}0\rangle$ crystal with a dielectric tensor where we substitute ε_{yy} by ε_{xx} and vice versa. We can also use the average $\frac{1}{2}(\varepsilon_{xx}+\varepsilon_{yy})$ for both. We find in any case that the optical response is very close to both the result obtained for the single crystal with the polarization vector along a main crystal axis and for the polycrystal. All these cases are much closer to each other than to the result for hcp $\langle 0001\rangle$; see also Fig. 5. The conclusion is that the difference between optical response of hcp $\langle 11\bar{2}0\rangle$ and hcp $\langle 0001\rangle$ is mainly due to the change in ε_{xy}. In this sense it may be regarded as an anisotropic polar MOKE or a manifestation of magnetocrystalline anisotropy in the optical response.

VII. POLAR MOKE OF CrO_2

A. Optical conductivity

We have calculated the optical conductivity tensor of $\langle 010\rangle$ CrO_2 with the first-principles approach as described in Sec. IV. The basis set was constructed from $4s4p3d$ and $4d4f$ (respectively, $2s2p$ and $3s3p$) orbitals for the chromium (respectively, oxygen) sites. The lattice constants and position parameters were $a=4.421$ Å, $c=2.916$ Å, and $x=0.3053$ as was used in Refs. 12 and 26–28. Here 32 768 **k** points were used to sample the Brillouin zone. Exchange correlation was treated in the same way as in the calculation for Co above.

The magnetic moment per CrO_2, $m=2.0\mu_B$, and total energy per unit cell as well as the density of states agree well with those given in Refs. 12, 18, and 28. Figure 6 shows our calculated optical conductivity tensor. Results are in good agreement with previous theoretical findings.[12,18]

B. Optical response of the polycrystal

If thin films of CrO_2 are deposited on single-crystalline Al_2O_3, polycrystalline growth is observed. Crystallites order sixfold symmetrically with an a axis oriented perpendicular to the surface.[29] Experimental results suggest that the sizes of crystallites in such films are typically of the order $0.1-10$ μm. For the lower limit we are in a regime where interference effects start to play a role. Consequently the optical response is no longer a purely incoherent wave and can in general *not* be described by average Stokes parameters. We exclude this case here. For the upper limit the

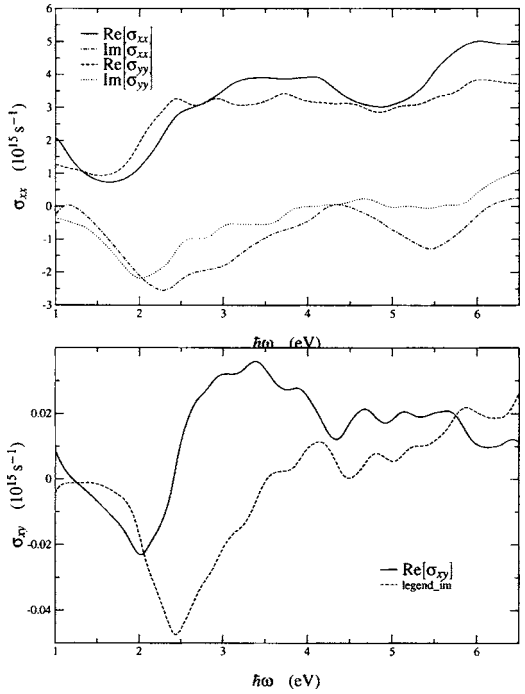

FIG. 6. Calculated optical conductivity tensor of $\langle 010\rangle$ CrO_2.

optical response of the polycrystal is well described by average Stokes parameters.

We have calculated the optical response of polycrystalline $\langle 010\rangle$ CrO_2 with sixfold symmetric domain ordering. We find that the optical response is independent of the direction of the polarization vector. Results are shown in Fig. 7. They are in good agreement with experimental data.

Also, the results are in good agreement with analytical findings given in Appendix A: the sixfold-symmetric polycrystal is a member of the isotropic class which implies that crystallographic birefringence is averaged out completely both in the rotation and in the ellipticity.

The results have an important implication. In a previous theoretical work Uspenskiĭ *et al.*[12] derived an approximative analytic expression for the polar MOKE of a polycrystalline surface with two-dimensional random domain distribution. It reads

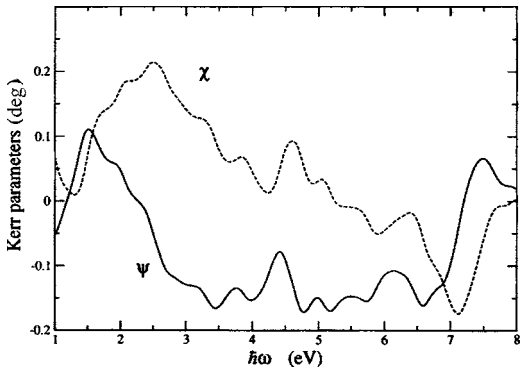

FIG. 7. Calculated optical response of *a*-axis-textured sixfold symmetrically ordered CrO_2. The solid line shows the rotation ψ of the polarization ellipse. The dashed line shows its ellipticity χ.

$$\psi + i\chi = \frac{2\varepsilon_{xy}}{(\sqrt{\varepsilon_{xx}} + \sqrt{\varepsilon_{yy}})(1 - \sqrt{\varepsilon_{xx}}\sqrt{\varepsilon_{yy}})}. \tag{33}$$

Here the roots are taken in the upper complex half plane. From the more recent experimental works[29] it is clear that domain distribution of polycrystalline CrO_2 is actually *not* random rather it has sixfold symmetry. So Eq. (33) is in general not applicable. However, from the analytical results of Appendix A we know now that the optical response of the sixfold-symmetric polycrystal is equivalent to the optical response of a random polycrystal of the same material. Thus, the validity of the approximative expression is extended to the whole isotropic class. Hence, indeed the optical response of CrO_2 can be calculated with Eq. (33).

We have calculated the optical response also with the approximative expression. Results differ from the rigorous result obtained with our transfer matrix calculation and subsequent determination of exact average Stokes parameters to the fourth relevant digit. This shows that (for CrO_2) the approximative expression is actually very good. Also it shows that the computational results are in very good agreement with the rigorous analytic treatment given in Appendix A.

VIII. SUMMARY AND CONCLUSION

We have calculated the polar magneto-optical Kerr effect for hcp $\langle 11\bar{2}0\rangle$ Co and for $\langle 010\rangle$ CrO_2. Our approach was based on first-principles calculations of dielectric tensors. We have addressed the electrodynamics part of the problem—i.e., the extraction of MOKE from dielectric tensors—with a transfer matrix method. We could describe the simultaneous occurrence of the birefringence and magnetic effects that is present in the systems. For polycrystals the average optical response was described by exact average Stokes parameters, taking into account the real orientations of domains.

For hcp $\langle 11\bar{2}0\rangle$ Co we found that a single-crystal optical response depends strongly on the direction of the polarization vector. If the polarization vector is along one of the main crystal axes, the optical response is very similar to the common polar MOKE and, moreover, for the two crystal axes the optical response is basically the same. If the polarization vector deviates more than about 3° from one of the main crystal axes, birefringence is important. For larger angles it dominates over the actual magnetic effect. To explain the experimental data we had to stress that the samples investigated in the experiment were polycrystals. We could show that already the presence of two domain orientations leads to a strong reduction of the birefringent contribution in the magneto-optical response. Finally we could show that the previous interpretation of experimental data in terms of a manifestation of magnetocrystalline anisotropy in the optical response remains valid.

For polycrystalline $\langle 010\rangle$ CrO_2 we found that the birefringent contribution to the optical response is averaged out completely. We could verify that a previous

approximative analytic expression describes the optical response exactly also for the case of realistic domain orientations.

The results of our local density approximation (LDA) calculations for both hcp Co and CrO_2 are in very good agreement with the experimental data (assuming that the data for Co are for a bicrystal). This is not trivial since, in general, correlation effects might be essential for the electronic structure of transition metal ferromagnets.[30] The effect of local Coulomb interactions on the magneto-optical properties of Fe and Ni has been calculated in Refs. 31 and 32 in the framework of a dynamical mean-field theory (LDA+DMFT approach). It appeared that, whereas for Ni the correlation effects are important, for Fe there are almost no difference between LDA and LDA+DMFT results for optical and magneto-optical properties. Our results show that probably correlation effects are not very important also for magneto-optical properties of Co. As for ferromagnetic CrO_2 a recent analysis[33] shows that it should be considered rather as a weakly correlated system, so the success of our calculations is not surprising.

ACKOWLEDGMENTS

We gratefully acknowledge stimulating discussions with Thorsten Andersen, Peter Oppeneer, and Till Burkert. This work was supported financially by the Deutscher Akademischer Austauschdienst, Germany, by the Studienstiftung der Deutschen Wirtschaft, Studienförderwerk Klaus Murmann, Germany, by the Center for Dynamical Processes, University of Uppsala, Sweden, by the Swedish Research Council (VR), the foundation for strategic research (SSF), and the Göran Gustafsson foundation.

APPENDIX A: CLASSIFICATION OF POLYCRYSTALLINE SURFACES

Most polycrystalline surfaces occurring in nature have either a three-dimensional distribution of domain orientations or a two-dimensional distribution with only few domain orientations that are related to each other by a rotation round the surface normal. The three-dimensional distribution is found for surfaces of bulk polycrystals such as, e.g., natural iron. The ordered two-dimensional distribution is often found when thin polycrystalline films are grown on single-crystalline substrates. In the case of the three-dimensional distribution, the domain orientations are often to a good approximation random. The average polar MOKE of a three-dimensional random polycrystal is obviously independent of the direction of the polarization vector in the surface plane. We skip this case here as well as other three-dimensionally ordered polycrystals. Rather we focus on polycrystals with a two-dimensional distribution of domain orientations. We call a surface n-fold symmetrically ordered if the crystallographic structures of all domains can be mapped onto each other by an n-fold rotation around the surface normal. We will also use a notion of a two-dimensional continuously distributed polycrystalline surface. By that we mean a polycrystalline surface in which the crystallographic structures of the domains can be mapped onto each other by suitable continuous rotations around the surface normal and all possible orientations occur. This corresponds to two-dimensional random domain orientations. Also for this case, the average polar MOKE is obviously independent of the direction of the polarization vector.

We show now that for most polycrystals with symmetrically ordered domains the average polar MOKE is equivalent to the average polar MOKE of a continuously distributed polycrystal of the same material.

In particular we prove the following statement. The average Stokes parameters $\langle S_0\rangle$ and $\langle S_3\rangle$ are identical to those of a continuous polycrystal if and only if the in-plane symmetry of domain orientations is larger than twofold and the Stokes parameters $\langle S_1\rangle$ and $\langle S_2\rangle$ are identical to those of a continuous polycrystal if and only if the in-plane symmetry of domain orientations is not 1, 2, or 4.

We begin the proof by considering the light reflected from a single domain. If reflection is described by means of a transfer matrix method, then, for any wave vector and frequency, the complex amplitude of the reflected wave is a linear mapping of the complex amplitude of the incident wave. This can be seen directly from the main linear equation (14). Further, in case of normal incidence, the incident and reflected amplitude vectors may be represented in a common coordinate system parallel to the surface plane. Thus, if $\boldsymbol{E}^{in}$ and $\boldsymbol{E}^{refl}$ are respective 2-vectors, there is a linear transformation $T:\mathbb{C}^2\to\mathbb{C}^2$ such that

$$\boldsymbol{E}^{refl} = T\boldsymbol{E}^{in}. \tag{A1}$$

Now let some other domain be identical to the previous one up to a rotation

$$R(\varphi) = \begin{pmatrix} \cos\varphi & \sin\varphi \\ -\sin\varphi & \cos\varphi \end{pmatrix} \tag{A2}$$

around the surface normal.

If $\boldsymbol{E}_2^{refl}$ is the amplitude of the wave reflected from the second domain, we have

$$\boldsymbol{E}_2^{refl} = R(\varphi)TR^{-1}(\varphi)\boldsymbol{E}^{in}. \tag{A3}$$

Now consider an n-fold symmetrically ordered polycrystal. Introducing the angles $\varphi_k = 2\pi k/n$, $k=1,\ldots,n$, the amplitude vectors $\boldsymbol{E}_k^{refl}$ of the reflected waves are

$$\boldsymbol{E}_k^{refl} = R(\varphi_k)TR^{-1}(\varphi_k)\boldsymbol{E}^{in}. \tag{A4}$$

By Eq. (15) the average Stokes parameters are

$$\langle \boldsymbol{S}\rangle = \sum_{k=1}^{n} \boldsymbol{S}\left[R\left(2\pi\frac{k}{n}\right)TR^{-1}\left(2\pi\frac{k}{n}\right)\boldsymbol{E}^{in}\right]. \tag{A5}$$

For a continuously distributed polycrystal we have

$$\langle \boldsymbol{S}\rangle = \frac{1}{2\pi}\int_0^{2\pi} \boldsymbol{S}[R(\varphi)TR^{-1}(\varphi)\boldsymbol{E}^{in}]d\varphi. \tag{A6}$$

It is shown in Appendix C that the latter two expressions are equal in the first and last component if and only if $n \notin \{1,2\}$

and in the second and third components if and only if $n \notin \{1,2,4\}$. This finishes the proof.

The latter statement is fundamental for the understanding of the average polar MOKE of polycrystals. It naturally decides thin polycrystalline films into three classes: twofold symmetrically ordered films, fourfold symmetrically ordered films, and all others including two-dimensional random orientation. Further, it implies that for polycrystalline films out of the first two classes the optical response does in general depend on the direction of the polarization vector. Thus the birefringent contribution to the optical response is in general *not* averaged out. On the other hand, it implies that for polycrystals out of the last class the optical response is independent of the direction of the polarization vector. Thus the birefringent contribution to the optical response *is* averaged out.

APPENDIX B: SYMMETRIC SUMS OVER POWERS OF TRIGONOMETRIC FUNCTIONS

We prove a statement about symmetric sums over powers of cos and sin.

Let $f:\mathbb{R}\to\mathbb{R}$ and $q\in\mathbb{Q}$. Then the identity

$$\frac{1}{2\pi}\int_0^{2\pi} f(x)dx = \frac{1}{n}\sum_{k=1}^{n} f\left(2\pi\frac{k}{n}\right) = q$$

holds for pairs f, q,

$$\cos^2, \quad \frac{1}{2},$$

$$\sin^2, \quad \frac{1}{2},$$

$$\cos \sin, \quad 0,$$

$$\cos^4 + \cos^2 \sin^2, \quad \frac{1}{2}\frac{3}{4} + \frac{1}{8},$$

$$\sin^4 + \cos^2 \sin^2, \quad \frac{1}{2}\frac{3}{4} + \frac{1}{8},$$

$$\cos^3 \sin + \sin^3 \cos, \quad 0,$$

$$\sin^4 - \cos^4, \quad 0, \tag{B1}$$

if and only if $n \notin \{1,2\}$, and for pairs f, q

$$\cos^4, \quad \frac{1}{2}\frac{3}{4},$$

$$\sin^4, \quad \frac{1}{2}\frac{3}{4},$$

$$\cos^2 \sin^2, \quad \frac{1}{8},$$

$$\cos^3 \sin, \quad 0,$$

$$\sin^3 \cos, \quad 0,$$

$$\cos^4 - \cos^2 \sin^2, \quad \frac{1}{2}\frac{3}{4} - \frac{1}{8},$$

$$\sin^4 - \cos^2 \sin^2, \quad \frac{1}{2}\frac{3}{4} - \frac{1}{8},$$

$$\cos^3 \sin - \sin^3 \cos, \quad 0, \tag{B2}$$

if and only if $n \notin \{1,2,4\}$.

We begin the proof by considering sums of the form

$$\frac{1}{n}\sum_{k=1}^{n} e^{mi2\pi k/n}, \quad m \in \mathbb{N}, \tag{B3}$$

where $n \in \mathbb{N}, n \geqslant 2$.

If $m=ln$ with some $l \in \mathbb{N}$, then

$$\frac{1}{n}\sum_{k=1}^{n} e^{mi2\pi k/n} = \frac{1}{n}\sum_{k=1}^{n} e^{li2\pi k} = 1, \tag{B4}$$

whereas if $n=lm$ with some $l \in \mathbb{N}$, we have

$$\frac{1}{n}\sum_{k=1}^{n} e^{mi2\pi k/n} = \frac{1}{n}\sum_{k=1}^{lm} e^{i2\pi k/l} = \frac{1}{n} m \sum_{k=1}^{l} e^{i2\pi k/l} = 0. \tag{B5}$$

Now let p and q be the largest prime numbers occurring in the prime factorizations of n and m, respectively. Let $\mathbb{F}_p=\{\{0,1,\ldots,p-1\},\cdot,+\}$ be the prime field of the modulo classes of p in the common sense. Let $m\cdot\mathbb{F}\subset\mathbb{N}$ be the set $\{0,1q\backslash p,2q\backslash p,\ldots,(p-1)q\backslash p\}$. We divide the set of complex numbers occurring in Eq. (B3) into s subsets. We chose s such that $n=s\cdot p$ and consider

$$A_j = \{e^{i2\pi(k/p)+mi2\pi j/n}, k \in m\cdot\mathbb{F}_p\}, \quad j=1,\ldots,s. \tag{B6}$$

Then

$$\begin{aligned}\frac{1}{n}\sum_{k=1}^{n} e^{mi2\pi k/n} &= \frac{1}{n}\left[\sum_{z\in A_1} + \cdots + \sum_{z\in A_s}\right] \\ &= \frac{1}{n}\left[(e^{mi2\pi(1/n)} + \cdots + e^{mi2\pi s/n}) \sum_{k\in m\cdot\mathbb{F}_p} e^{i2\pi k/p}\right] \\ &= 0 \text{ if } q < p. \end{aligned} \tag{B7}$$

Using Eqs. (B4), (B5), and (B7), we can calculate the sum given by Eq. (B3) with some $m \in \mathbb{N}$ for any $n \in \mathbb{N}$. We consider the cases $m=2$ and $m=4$.

For $m=2$ we obviously have a largest prime factor $q=2$; i.e., by Eq. (B7) the sum vanishes for

$$n = 3,6,7,9,10,11,12,\ldots$$

and any other natural number containing a prime greater than or equal to 3 in its factorization. For $n=4,8,16,\ldots$, the sum vanishes by Eq. (B5), while for $n=1,2$ the sum is one by Eq. (B4). Thus we have

$$\frac{1}{n}\sum_{k=1}^{n} e^{2i2\pi k/n} = 0 \quad \text{if and only if} \quad n \notin \{1,2\}. \tag{B8}$$

For $m=4$, we have a largest prime factor $q=2$ as well; i.e., the sum vanishes again for

$$n = 3,6,7,9,10,11,12,\ldots$$

and any other natural number containing a prime greater than or equal to 3 in its factorization. For $n=8,16,32,\ldots$, the sum vanishes by Eq. (B5), while for $n=1,2,4$, we obtain by Eq. (B4) that the sum is one. Thus

$$\frac{1}{n}\sum_{k=1}^{n} e^{4i2\pi k/n} = 0 \quad \text{if and only if} \quad n \notin \{1,2,4\}. \tag{B9}$$

We prove the first line of Eq. (B1). The identity

$$\frac{1}{2\pi}\int_0^{2\pi} \cos^2(\varphi)d\varphi = \frac{1}{2} \tag{B10}$$

follows from the more general formula

$$\int_0^{\pi/2} \sin^{2\alpha+1}(\varphi)\cos^{2\beta+1}(\varphi)d\varphi = \frac{\Gamma(\alpha+1)\Gamma(\beta+1)}{2\Gamma(\alpha+1+\beta+1)}, \tag{B11}$$

where Γ is the gamma function.[34] Further,

$$\begin{aligned}\frac{1}{n}\sum_{k=1}^{n} \cos^2\left(2\pi\frac{k}{n}\right) &= \frac{1}{2} + \frac{1}{n}\frac{1}{4}\sum_{k=1}^{n}\left[e^{2i2\pi k/n} + e^{-2i2\pi k/n}\right] \\ &= \frac{1}{2} \quad \text{if and only if} \quad n \notin \{1,2\},\end{aligned} \tag{B12}$$

where we have used Eq. (B8) for the last line.

In a similar way, the second and third lines of Eq. (B1) follow from Eqs. (B11) and (B8).

Next we prove the first line of Eq. (B2). Once again, we refer to Eq. (B11) to see that

$$\frac{1}{2\pi}\int_0^{2\pi} \cos^4(\varphi)d\varphi = \frac{1}{2}\frac{3}{4}. \tag{B13}$$

On the other hand,

$$\begin{aligned}\frac{1}{n}\sum_{k=1}^{n} \cos^4\left(2\pi\frac{k}{n}\right) &= \frac{1}{2}\frac{3}{4} + \frac{1}{n}\frac{1}{16}\sum_{k=1}^{n}\left[e^{4i2\pi k/n} + e^{-4i2\pi k/n}\right. \\ &\quad \left. + 4e^{2i2\pi k/n} + 4e^{-2i2\pi k/n}\right] \\ &= \frac{1}{2}\frac{3}{4} \quad \text{if and only if} \quad n \notin \{1,2,4\},\end{aligned} \tag{B14}$$

where we have used Eqs. (B8) and (B9) for the last line.

In a similar way, we find

$$\frac{1}{n}\sum_{k=1}^{n} \sin^4\left(2\pi\frac{k}{n}\right) = \frac{1}{2}\frac{3}{4}, \tag{B15}$$

$$\frac{1}{n}\sum_{k=1}^{n} \cos^2\left(2\pi\frac{k}{n}\right)\sin^2\left(2\pi\frac{k}{n}\right) = \frac{1}{8}, \tag{B16}$$

$$\frac{1}{n}\sum_{k=1}^{n} \cos^3\left(2\pi\frac{k}{n}\right)\sin\left(2\pi\frac{k}{n}\right) = 0, \tag{B17}$$

and

$$\frac{1}{n}\sum_{k=1}^{n} \cos\left(2\pi\frac{k}{n}\right)\sin^3\left(2\pi\frac{k}{n}\right) = 0, \tag{B18}$$

if and only if $n \notin \{1,2,4\}$. This gives the first five identities of Eq. (B2).

To see that the last four lines of Eq. (B1) hold, we add the corresponding expressions obtained above and find that in all cases the sums over fourth powers cancel, while sums over second powers remain. In contrast to that, also the fourth-order sums remain in the expressions for the last three lines of Eq. (B2). This finishes the proof.

APPENDIX C: AVERAGE STOKES PARAMETERS FOR n-FOLD-ROTATED 2×2 LINEAR TRANSFORMATIONS

Let $\boldsymbol{E} \in \mathbb{R}^2$, $R(\varphi):\mathbb{R}^2 \to \mathbb{R}^2$ be a rotation by an angle φ and $T:\mathbb{C}^2 \to \mathbb{C}^2$ a linear transformation of most general symmetry. Let $S_j:\mathbb{C}^2 \to \mathbb{R}$, $j=0,1,2,3$ be the Stokes parameters. Then

$$\begin{aligned}\frac{1}{n}\sum_{k=1}^{n} S_j\left[R\left(2\pi\frac{k}{n}\right)TR\left(2\pi\frac{k}{n}\right)^{-1}\boldsymbol{E}\right] \\ = \frac{1}{2\pi}\int_0^{2\pi} S_j[R(\varphi)TR^{-1}(\varphi)\boldsymbol{E}]d\varphi\end{aligned} \tag{C1}$$

holds for $j=0,3$ if and only if $n \notin \{1,2\}$ and for $j=1,2$ if and only if $n \notin \{1,2,4\}$.

We treat the four cases separately.

Consider S_0.

First we evaluate the expression for the Stokes parameter occurring in Eq. (C1). Dropping the angular argument of the rotation, we get from Eq. (15)

$$\begin{aligned}S_0(RTR^{-1}\boldsymbol{E}) &= [RTR^{-1}\boldsymbol{E}]_x\overline{[RTR^{-1}\boldsymbol{E}]}_x + [RTR^{-1}\boldsymbol{E}]_y\overline{[RTR^{-1}\boldsymbol{E}]}_y \\ &= (RTR^{-1}\boldsymbol{E}, RTR^{-1}\boldsymbol{E}),\end{aligned} \tag{C2}$$

where $(\cdot,\cdot)$ denotes the standard scalar product in $\mathbb{C}^2$. R is orthogonal, thus

$$(RTR^{-1}\boldsymbol{E}, RTR^{-1}\boldsymbol{E}) = (TR^{-1}\boldsymbol{E}, TR^{-1}\boldsymbol{E}), \tag{C3}$$

which expresses, that in a total intensity measurement, the reflected light of a polycrystal illuminated with a single incident beam is not distinguishable from the reflected light of a single crystal illuminated with several beams with respective orientations of the polarization vectors. We denote $c=\cos(\varphi)$, $s=\sin(\varphi)$, and

$$R = \begin{pmatrix} c & s \\ -s & c \end{pmatrix}. \tag{C4}$$

Thus

$$TR^{-1} = \begin{pmatrix} cT_{xx} + sT_{xy} & -sT_{xx} + cT_{xy} \\ cT_{yx} + sT_{yy} & -sT_{yx} + cT_{yy} \end{pmatrix}. \tag{C5}$$

Introducing $\boldsymbol{E} = (a,b)$, we have

$$\begin{aligned}
[TR^{-1}\boldsymbol{E}]_x\overline{[TR^{-1}\boldsymbol{E}]}_x &= [(cT_{xx} + sT_{xy})a + (-sT_{xx} + cT_{xy})b]\overline{[(cT_{xx} + sT_{xy})a + (-sT_{xx} + cT_{xy})b]} \\
&= (c^2T_{xx}\bar{T}_{xx} + csT_{xx}\bar{T}_{xy} + csT_{xy}\bar{T}_{xx} + s^2T_{xy}\bar{T}_{xy})a^2 \\
&\quad + (-csT_{xx}\bar{T}_{xx} + c^2T_{xx}\bar{T}_{xy} - s^2T_{xy}\bar{T}_{xx} + csT_{xy}\bar{T}_{xy})a^2 + (-scT_{xx}\bar{T}_{xx} - s^2T_{xx}\bar{T}_{xy} + c^2T_{xy}\bar{T}_{xx} + csT_{xy}\bar{T}_{xy})a^2 \\
&\quad + (s^2T_{xx}\bar{T}_{xx} - scT_{xx}\bar{T}_{xy} - scT_{xy}\bar{T}_{xx} + c^2T_{xy}\bar{T}_{xy})a^2.
\end{aligned} \tag{C6}$$

Thus by the first three lines of Eq. (B1)

$$\frac{1}{2\pi}\int_0^{2\pi} [TR^{-1}(\varphi)\boldsymbol{E}]_x\overline{[TR^{-1}(\varphi)\boldsymbol{E}]}_x d\varphi = \frac{1}{n}\sum_{k=1}^{n}\left[TR^{-1}\left(2\pi\frac{k}{n}\right)\boldsymbol{E}\right]_x\overline{\left[TR^{-1}\left(2\pi\frac{k}{n}\right)\boldsymbol{E}\right]}_x \tag{C7}$$

if and only if $n \notin \{1,2\}$. From Eq. (C5) we see, that the y component of the transformed vector has the same form as the x component. This completes the proof for S_0.

Consider S_1 and S_2.

In contrast to S_0, both S_1 and S_2 are no scalar products. Thus, we have to evaluate the full expression $RTR^{-1}\boldsymbol{E}$. With Eqs. (C4) and (C5) we get

$$RTR^{-1} = \begin{pmatrix} c^2T_{xx} + csT_{xy} + csT_{yx} + s^2T_{yy} & -csT_{xx} + c^2T_{xy} - s^2T_{yx} + csT_{yy} \\ -csT_{xx} - s^2T_{xy} + c^2T_{yx} + csT_{yy} & s^2T_{xx} - csT_{xy} - scT_{yx} + c^2T_{yy} \end{pmatrix}. \tag{C8}$$

We denote $\mathbb{E} = (a,b)$ as before and $RTR^{-1}\boldsymbol{E} = \boldsymbol{E}' = (E'_x, E'_y)$. Then

$$\begin{aligned}
E'_x &= (c^2T_{xx} + csT_{xy} + csT_{yx} + s^2T_{yy})a \\
&\quad + (-csT_{xx} + c^2T_{xy} - s^2T_{yx} + csT_{yy})b, \\
E'_y &= (-csT_{xx} - s^2T_{xy} + c^2T_{yx} + csT_{yy})a \\
&\quad + (s^2T_{xx} - csT_{xy} - csT_{yx} + c^2T_{yy})b.
\end{aligned} \tag{C9}$$

By Eq. (15), we have

$$S_1 = E'_x\overline{E'}_x - E'_y\overline{E'}_y \tag{C10}$$

and

$$S_2 = E'_x\overline{E'}_y + \overline{E'}_xE'_y. \tag{C11}$$

If we evaluate these expressions by substituting Eq. (C9), every resulting term contains factors of cos and sin of the form considered in Eq. (B1) or (B2). These terms might add up to combined terms out of the last four lines of Eq. (B1) or the last three lines of Eq. (B2). To check, if we have at least one independent term out of Eq. (B2), we focus on expressions with a factor $T_{xx}\bar{T}_{xx}$. We obtain

$$\begin{aligned}
S_1 &= T_{xx}\bar{T}_{xx}(c^4a^2 - c^3sab + c^2s^2b^2 - c^2s^2a \\
&\quad + cs^3ab - s^4b^2) + \cdots \\
&= T_{xx}\bar{T}_{xx}[(c^4 - c^2s^2)a^2 - (s^2c^2 - s^4)b^2 \\
&\quad + (cs^3 - c^3s)ab] + \cdots
\end{aligned} \tag{C12}$$

and

$$S_2 = 2T_{xx}\bar{T}_{xx}(c^3sa^2 + 2c^2s^2ab - cs^3b^2) + \cdots. \tag{C13}$$

Thus, we have independent terms out of Eq. (B2) which cannot be combined to terms out of Eq. (B1). This proves the cases S_1 and S_2.

Last consider S_3.

Using the same notation as before and the results obtained in Eq. (C9), we have

$$\begin{aligned}
E'_x\overline{E'}_y &= [-c^3sT_{xx}\bar{T}_{xx} - c^2s^2T_{xx}\bar{T}_{xy} + c^4T_{xx}\bar{T}_{yx} + c^3sT_{xx}\bar{T}_{yy} - c^2s^2T_{xy}\bar{T}_{xx} - cs^3T_{xy}\bar{T}_{xy} + c^3sT_{xy}\bar{T}_{yx} + c^2s^2T_{xy}\bar{T}_{yy} - c^2s^2T_{yx}\bar{T}_{xx} \\
&\quad - cs^3T_{yx}\bar{T}_{xy} + c^3sT_{yx}\bar{T}_{yx} + c^2s^2T_{yx}\bar{T}_{yy} - c^2s^2T_{yy}\bar{T}_{xx} - cs^3T_{yy}\bar{T}_{xy} + c^3sT_{yy}\bar{T}_{yx} + c^2s^2T_{yy}\bar{T}_{yy}]a^2 + [c^2s^2T_{xx}\bar{T}_{xx} - c^3sT_{xx}\bar{T}_{xy} \\
&\quad - c^3sT_{xx}\bar{T}_{yx} + c^4T_{xx}\bar{T}_{yy} + cs^3T_{xy}\bar{T}_{xx} - c^2s^2T_{xy}\bar{T}_{xy} - c^2s^2T_{xy}\bar{T}_{yx} + c^3sT_{xy}\bar{T}_{yy} + cs^3T_{yx}\bar{T}_{xx} - c^2s^2T_{yx}\bar{T}_{xy} - c^2s^2T_{yx}\bar{T}_{yx}
\end{aligned}$$

$$+c^3sT_{yx}\bar{T}_{yy}+s^4T_{yy}\bar{T}_{xx}-cs^3T_{yy}\bar{T}_{xy}-cs^3T_{yy}\bar{T}_{yx}+c^2s^2T_{yy}\bar{T}_{yy}+c^2s^2T_{xx}\bar{T}_{xx}+c^3sT_{xx}\bar{T}_{xy}-c^3sT_{xx}\bar{T}_{yx}-c^2s^2T_{xx}\bar{T}_{yy}$$
$$-c^3sT_{xy}\bar{T}_{xx}-c^2s^2T_{xy}\bar{T}_{xy}+c^4T_{xy}\bar{T}_{yx}+c^3sT_{xy}\bar{T}_{yy}+cs^3T_{yx}\bar{T}_{xx}+s^4T_{yx}\bar{T}_{xy}-c^2s^2T_{yx}\bar{T}_{yx}-cs^3T_{yx}\bar{T}_{yy}-c^2s^2T_{yy}\bar{T}_{xx}-cs^3T_{yy}\bar{T}_{xy}$$
$$+c^3sT_{yy}\bar{T}_{yx}+c^2s^2T_{yy}\bar{T}_{yy}]ab+[-cs^3T_{xx}\bar{T}_{xx}+c^2s^2T_{xx}\bar{T}_{xy}+c^2s^2T_{xx}\bar{T}_{yx}-c^3sT_{xx}\bar{T}_{yy}+c^2s^2T_{xy}\bar{T}_{xx}-c^3sT_{xy}\bar{T}_{xy}-c^3sT_{xy}\bar{T}_{yx}$$
$$+c^4T_{xy}\bar{T}_{yy}-s^4T_{yx}\bar{T}_{xx}+cs^3T_{yx}\bar{T}_{xy}+cs^3T_{yx}\bar{T}_{yx}-c^2s^2T_{yx}\bar{T}_{yy}+cs^3T_{yy}\bar{T}_{xx}-c^2s^2T_{yy}\bar{T}_{xy}-c^2s^2T_{yy}\bar{T}_{yx}+c^3sT_{yy}\bar{T}_{yy}]b^2.$$

With Eq. (15) we obtain

$$S_3=i(E'_x\overline{E'}_y-\overline{E'}_xE'_y)$$
$$=[(c^4+c^2s^2)T_{xx}\bar{T}_{xx}-(c^4+c^2s^2)T_{yx}\bar{T}_{xx}+(c^3s+cs^3)T_{xx}\bar{T}_{yy}-(c^3s+cs^3)T_{yy}\bar{T}_{xx}-(s^4+c^2s^2)T_{yy}\bar{T}_{xy}+(s^4+c^2s^2)T_{xy}\bar{T}_{yy}$$
$$+(c^3s+cs^3)T_{xy}\bar{T}_{yx}-(c^3s+cs^3)T_{yx}\bar{T}_{xy}]a^2+[2[(c^3s+cs^3)T_{yx}\bar{T}_{xx}-(c^3s+cs^3)T_{xx}\bar{T}_{yy}]+2[(c^3s+cs^3)T_{xy}\bar{T}_{yy}$$
$$-(c^3s+cs^3)T_{yy}\bar{T}_{xy}]+(c^4+c^2s^2)T_{xx}\bar{T}_{yy}-(c^2s^2+c^4)T_{yy}\bar{T}_{xx}+(s^4+c^2s^2)T_{yy}\bar{T}_{xx}-(c^2s^2+s^4)T_{xy}\bar{T}_{yy}$$
$$+(c^4-s^4)T_{xy}\bar{T}_{yx}+(s^4-c^4)T_{yx}\bar{T}_{xy}]ab+[(c^2s^2+s^4)T_{xx}\bar{T}_{yx}-(s^4+c^2s^2)T_{yx}\bar{T}_{xx}+(cs^3+c^3s)T_{yx}\bar{T}_{xy}$$
$$-(c^3s+cs^3)T_{xy}\bar{T}_{yx}+(cs^3+c^3s)T_{xx}\bar{T}_{yy}-(c^3s+cs^3)T_{xx}\bar{T}_{yy}+(c^4+c^2s^2)T_{xy}\bar{T}_{yy}-(c^2s^2+c^4)T_{yy}\bar{T}_{yx}]b^2.$$

Indeed all terms contain a factor of cos and sin out of those given in Eq. (B1). This finishes the proof.

*Electronic address: helmut.rathgen@web.de

[1] D. Weller, G. R. Harp, R. F. C. Farrow, A. Cebollada, and J. Sticht, Phys. Rev. Lett. **72**, 2097 (1994).
[2] R. Kubo, J. Phys. Soc. Jpn. **12**, 570 (1957).
[3] D. A. Greenwood, Proc. Phys. Soc. London **71**, 585 (1958).
[4] C. S. Wang and J. Callaway, Phys. Rev. B **9**, 4897 (1974).
[5] P. N. Argyres, Phys. Rev. **97**, 334 (1955).
[6] M. Born and E. Wolf, *Principles of Optics*, 6th ed. (Pergamon Press, New York, 1980).
[7] J. Zak, C. Liu, E. R. Moog, and S. D. Bader, J. Appl. Phys. **68**, 4203 (1990).
[8] S. A. Stepanov and S. K. Sinha, Phys. Rev. B **61**, 15302 (2000).
[9] E. Anderson *et al.*, *LAPACK User's Guide*, 3rd ed. (SIAM, Philadelphia, 1999), http:\\www.netlib.org\lapack\lug\lapack_lug.html
[10] W. H. Press, B. P. Flannery, S. A. Teukolsky, and W. T. Vetter, *Numerical Recipes—The Art of Scientific Computing* (Cambridge University Press, Cambridge, England, 1986).
[11] H. Rathgen, Master's thesis, Technische Universität Braunschweig, 2003.
[12] Y. A. Uspenskiĭ, E. T. Kulatov, and S. V. Halilov, Phys. Rev. B **54**, 474 (1996).
[13] H. Rathgen and M. I. Katsnelson, Phys. Scr. **T109**, 170 (2004).
[14] P. M. Oppeneer, T. Maurer, J. Sticht, and J. Kübler, Phys. Rev. B **45**, 10924 (1992).
[15] T. Gasche, M. S. S. Brooks, and B. Johansson, Phys. Rev. B **53**, 296 (1996).
[16] P. Blaha, K. Schwarz, G. K. H. Madsen, D. Kvasnicka, and J. Luitz, Computer code WIEN2K, University Prof. Karlheinz Schwarz, Technical Universität Wien, Austria, 2001.
[17] H. Ebert, Rep. Prog. Phys. **59**, 1665 (1996).
[18] J. Kuneš, P. Novák, P. M. Oppeneer, C. König, M. Fraune, U. Rüdiger, G. Güntherodt, and C. Ambrosch-Draxl, Phys. Rev. B **65**, 165105 (2002).
[19] E. G. Maksimov, I. I. Mazin, S. N. Rashkeev, and Y. A. Uspenskii, J. Phys. F: Met. Phys. **18**, 833 (1988).
[20] J. M. Wills, O. Eriksson, M. Alouani, and D. L. Price, in *Electronic Structure and Physical Properties of Solid: The Uses of the LMTO Method*, edited by H. Dreyssé (Springer, Berlin, 2000), Chap. I, pp. 148–167.
[21] D. D. Koelling and B. N. Harmon, J. Phys. C **10**, 3107 (1977).
[22] R. R. Birss, Rep. Prog. Phys. **26**, 307 (1963).
[23] G. Y. Guo and H. Ebert, Phys. Rev. B **50**, 10377 (1994).
[24] P. M. Oppeneer, T. Kraft, and H. Eschrig, J. Magn. Magn. Mater. **148**, 298 (1995).
[25] U. von Barth and L. Hedin, J. Phys. C **5**, 1629 (1972).
[26] B. J. Thamer, R. M. Douglas, and E. Staritzky, J. Am. Chem. Soc. **79**, 547 (1957).
[27] K. Schwarz, J. Phys. F: Met. Phys. **16**, 211 (1986).
[28] S. Matar, G. Demazeau, J. Sticht, V. Eyert, and J. Kübler, J. Phys. I **2**, 315 (1992).
[29] M. Rabe, J. Pommer, K. Samm, B. Özyilmaz, C. König, M. Fraume, U. Rüdiger, G. Güntherodt, S. Senz, and D. Hesse, J. Phys.: Condens. Matter **14**, 7 (2002).
[30] A. I. Lichtenstein, M. I. Katsnelson, and G. Kotliar, Phys. Rev. Lett. **87**, 067205 (2001).
[31] A. Perlov, S. Chadov, H. Ebert, L. Chioncel, A. I. Lichtenstein, and M. I. Katsnelson, J. Magn. Magn. Mater. **272–276**, 523 (2004).
[32] A. Perlov, S. Chadov, H. Ebert, L. Chioncel, A. Lichtenstein, and M. Katsnelson, in *Physics of Spin in Solids: Materials, Methods and Applications*, edited by S. Halilov (Kluwer, Dordrecht, 2004), p. 161.
[33] A. Toropova, G. Kotliar, S. Y. Savrasov, and V. Oudovenko, cond-mat/0409554 (unpublished).
[34] I. N. Bronstein, K. A. Semendjajev, G. Musiol, and H. Mühling, *Taschenbuch der Mathematik*, 4th ed. (Verlag Harri Deutsch, 1999).